DOI: 10.1002/zaac.200801394

Synthesis and Characterization of Hybrid Materials Derived from Polyaniline and Lacunary Keggin-type Polyoxotungstates

Emmanuel F. C. Chimamkpam,[a] Firasat Hussain,[a] Andreas Engel,[b] Andreas Schilling,[b] and Greta R. Patzke*[a]

Dedicated to Professor Reinhard Nesper on the Occasion of His 60th Birthday

Keywords: Hybrid materials; Nanostructures; Conductive polymers; Polyoxometalates; Synthetic methods

Abstract. Organic-inorganic hybrid materials are an upcoming class of materials that attract increasing research interest. In the present manuscript, we report on the combination of a particularly versatile organic matrix – the conductive polymer polyaniline (PAni) – with a special type of polyoxometalates (POMs), namely a lacunary Keggin anion, $[AsW_9O_{33}]^{9-}$. Although the high application potential and the manifold structural motifs of POMs provide an almost infinite number of options for composite materials, up to now, only few POM-polymer combinations have been explored in more detail. Thus, we have investigated the interaction of PAni with the unique reactivity of $[AsW_9O_{33}]^{9-}$ that combines building-block facilities with the presence of a lone pair on the heteroatom. The resulting composite material was characterized with a wide spectrum of analytical techniques and the effect on the reaction conditions on the nanoscale structuring was investigated. Furthermore, the newly synthesized POM-PAni composites display a stable temperature-dependent resistivity that renders them promising for further applications.

Introduction

Nanostructured hybrids of conducting polymers and inorganic nanoparticles attract considerable attention in electro-optical and magnetic applications, where their inherent properties undergo nanoscale synergies to bring forward a new class of multipurpose materials with enhanced functionality and efficiency [1, 2]. Generally, the development of organic-inorganic hybrid materials and a vivid understanding of their submicrometer behavior remains a multidisciplinary challenge [3–5]. Polyaniline (PAni) is one such conducting polymer that has been extensively studied for the formation of composite materials due to its attributes of interest such as lightweight, low cost, good environmental stability, tunable structural, optical and electronic properties. This renders PAni important for potential applications in sensors [6], light-emitting diodes [7], electromagnetic interference shielding [8], fuel cells [9] and field-effect transistors [10]. Most of the studied and documented hybrids of PAni are composed of oxides of various elements across the periodic table. Recently, hybrids of PAni and polyoxometalates (POMs) have attracted the interest of some research groups because of their technological relevance, for example in capacitors [11] or electrocatalytic systems [12]. POMs are transition metal oxide clusters that are preferably formed from Mo, W, V, Nb and Ta in their high oxidation states. Their rich structural chemistry leads to a multitude of POM-based molecular architectures with a high application potential, e.g. in electrochemistry, catalysis and for biomedicinal tasks, and their potential as inorganic components in polymer-based hybrid materials is just about to be explored [13–16], as well as their combination with inorganic nanoparticles to form composites [17]. The Keggin-type POMs display a quite well-known structural motif that is composed of a tetrahedrally coordinated central hetero atom surrounded by four W_3O_{13} groups (triads) that are connected in a corner-sharing fashion via oxygen atoms (e.g. $[(PO_4)W_{12}O_{36}]^{3-}$) [18, 19]. Most of the studies on PAni-POM systems have been focused on the use of Keggin-type POMs as proton donors for the preparation of PAni [11, 20–23] or on the redox properties of the POMs [24]. Recently, molecular hybrids of the PAni/$H_3PM_{12}O_{40}$ (M = W, Mo) type as well as PAni/$H_4SiW_{12}O_{40}$ have been investigated for the development of solid-state electrochemical supercapacitors [11]. Table 1 provides a literature survey of the POMs that have been combined with PAni into hybrid composite materials: The majority of studies has been focused on classical Keggin-type POMs, whereas the multi-

* Prof. Dr. G. R. Patzke
Fax: +41-44-635-6802
E-Mail: greta.patzke@aci.uzh.ch
[a] University of Zurich
Institute of Inorganic Chemistry
Winterthurerstrasse 190
8057 Zurich, Switzerland
[b] University of Zurich
Institute of Physics
Winterthurerstrasse 190
8057 Zurich, Switzerland

Supporting information for this article is available on the WWW under **www.zaac.wiley-vch.de** or from the author.

Zeitschrift für anorganische und allgemeine Chemie ZAAC Journal of Inorganic and General Chemistry

Table 1. Literature survey of POM-PAni composites.

POM	Scope	Lit.
$[XW_{12}O_{40}]^{n-}$ (X = Si, P, Mo)	Conductivity, electrochemical and electrocatalytic properties	[25]
	Solid-state electrochemical supercapacitors	[11, 21]
$PMo_{12}O_{40}^{3-}$	Chemical polymerization of polyaniline and polypyrrole	[26]
	Application as cation-insertion electrodes	[27]
	Mono- and mulitlayers of ultrathin PAni	[28]
	Hybrid materials for energy storage in electrochemical capacitors	[22]
	Composites with embedded metal nanoparticles	[24]
α-$[SiW_{12}O_{40}]^{4-}$	Self-assembled multilayer films	[29]
$H_4SiW_{12}O_{40}$	Formation of PAni nanotubes	[20]
$H_4PMo_{11}VO_{40}$, $H_5PMo_{10}V_2O_{40}$, $H_6PMo_9V_3O_{40}$	Electrochemical behavior of doped PAni films	[30]
$H_4SiMo_{12}O_{40}$, $Na_6P_2Mo_{18}O_{62}$, $K_6P_2W_{18}O_{62}$, α_1-$K_7P_2W_{17}VO_{62}$	Electrocatalytic reduction of nitrite and nitric oxide	[12]

tude of other POM types still remains to be investigated with respect to their incorporation into PAni matrices.

As for the remaining POM-polymer systems described in the literature, poly(allylamine hydrochloride) (PAH) is another frequently used matrix material that has, for example, been combined with the selected rare-earth containing tungstates [31], as well as with specific large polyoxomolybdates of the "Keplerate" type [32]. The majority of functional POM types, such as lacunary Keggin-type derivatives, however, have not been subjected to polymer composite formation. Lacunary Keggin structures are derived from the parent type by the removal of specific WO_6 moieties, followed by an optional rotation of the remaining WO_6 octahedra [12, 33]. As a consequence, these highly reactive POM fragments attract increasing research interest, e.g. as building blocks for large lanthanide-containing POMs [34] and for the study of their self assembly processes [35]. Furthermore, the presence of a free electron pair on the heteroatom provides special facilities for the construction of open and flexible POM architectures.

In this work, we therefore report for the first time on the incorporation of a lacunary Keggin POM, nonatungstoarsenate(III), α-$[AsW_9O_{33}]^{9-}$, into the PAni matrix. The α-$[AsW_9O_{33}]^{9-}$ anion bears a lone pair of electrons on the central hetero atom, and it displays a higher charge than most of the protonated POMs that have been used in previous studies [11, 20–23]. Thus, its unique open structural features in combination with a high charge density and electron-donor properties render α-$[AsW_9O_{33}]^{9-}$ an interesting candidate for the formation of organic-inorganic hybrid materials from conductive polymers. Nevertheless, the use of the reactive lacunary anion $[AsW_9O_{33}]^{9-}$ as a component of PAni-derived hybrid materials has not been explored so that the present study has been undertaken to investigate new modes of interaction between a lone pair-containing POM and a conductive polymer. Our results reveal that $[AsW_9O_{33}]^{9-}$ can modify the inherent properties of PAni as well as template the morphology of the polymer. This provides us a bedrock for the future incorporation of large complex and functionalized POMs derived from such building blocks that are currently prepared and investigated in our group.

Results and Discussion

Synthesis

In the following, we discuss the synthesis and characterization of hybrid materials obtained from PAni and the lacunary POM α-$[AsW_9O_{33}]^{9-}$. The typical synthesis entails the devised preparation of pristine PAni in both aqueous and acidic media. To ensure homogeneous doping of the same counter anion in the acidic medium, we used sulfuric acid (0.5 M) since it emanates as a by-product of PAni synthesis. During the synthesis, two phases are formed in the water system prior to the initiation stage, whereas the acidic system is single-phase due to the formation of hydrophilic anilinium sulfates. A solution of the initiator prepared from the respective media is added to start the polymerization. On injection of the oxidant initiator, a brown, monophasic solution that changes to dark green within 15 minutes is formed in the water system. In the acidic system, a colorless, yet one-phase solution is produced: It transforms to short-lived violet, then to blue and finally to a dark green colored solution, all within 5 to 20 minutes. The polymerization is allowed to proceed for 2–6 hours. During the purification stage, water was used to wash the products several times until the filtrate became very clear. Nevertheless, after drying at 65 °C for 72 hours, some quantities of the products (the solvent: polymer ratio does not have to be fixed) were soaked in chloroform ($CHCl_3$) for about 6 hours and subsequently washed repeatedly with the organic solvent to get a clear filtrate. $CHCl_3$ is chemically inert with respect to PAni, and it is therefore presumed to remove low molecular weight compounds present in the products [36]. This step was taken in order to check for the necessity and influence of the extra purification step on the materials' properties after thorough washing of the products with deionized water. For the preparation of the hybrid material, a facile route for the incorporation of $[AsW_9O_{33}]^{9-}$ in the PAni matrix is provided both in aqueous and acidic media. In a typical synthesis in the aqueous medium, the monomer is added to a clear solution of $[AsW_9O_{33}]^{9-}$. In this system, weak hydrogen bonding probably ensues between the monomer and the inorganic particles. In contrast, the positively charged anilinium ions formed in the acidic medium

electrostatically couple with the negatively charged $[AsW_9O_{33}]^{9-}$, thereby creating a very strong interaction between the monomer and the inorganic particles. The strong interactive force fosters very close contact interfaces between the incorporated nonatungstoarsenate(III) and the PAni matrix after polymerization. However, a yellow color observed in the acidic solution of $[AsW_9O_{33}]^{9-}$ could be indicating the isomerization of α-$[AsW_9O_{33}]^{9-}$ that is stable in the pH range from 4−8 into the β-isomer that exists at pH values around 2−0 [37, 38]. The polymerization and purification of the hybrids was carried out akin to the pristine PAni.

Spectroscopic Characterization

The FTIR spectra of the polymerized samples reveal that further purification with $CHCl_3$ has no significant influence on the pristine and hybrid polymer obtained from the acidic medium (see Supporting Information, Figure 1s). In contrast, the spectra of the samples obtained from the aqueous system show disappearance and/or great diminution of bands that are attributed to low molecular weight compounds (e.g. 695 cm^{-1}, 739 cm^{-1}, 759 cm^{-1}, 1414 cm^{-1}) [36], which are preferably formed in the water system. Apart from an additional band of the water-based product at 1041 cm^{-1}, assigned to C−H in-plane bending of 1, 2, 4-ring, no pronounced differences are observed between the spectra of akin products obtained from the different reaction systems, indicating that the main components of each specimen have similar chemical structures.

In Figure 1a, pristine PAni exhibits characteristic bands at 509 cm^{-1}, 826 cm^{-1}, 1149 cm^{-1}, 1303 cm^{-1}, 1499 cm^{-1} and 1583 cm^{-1} (1). The bands at 509 cm^{-1} and 826 cm^{-1} are assigned to aromatic ring deformation and C−H out-of-plane bending of 1−4 ring, respectively. The broad and intense band at 1149 cm^{-1} corresponds to the N=Q=N stretching mode (Q represents quinoid ring), which is associated with electron delocalization and electrical conductivity, and it is indicative of PAni protonation. The band at 1303 cm^{-1} is attributed to the C−N stretching in secondary aromatic amines (QBcQ, QBB, BBQ; where B signifies benzenoid ring and c represents cis) while the bands at 1499 cm^{-1} and 1583 cm^{-1} are associated with the C−C stretching in benzenoid ring (N−B−N) and C=C stretching in quinoid ring (N=Q=N), respectively [39]. The emergence of new bands, typical of tungstoarsenate(III) polyanions, in the spectra of the hybrids obtained from the different reaction systems indicates a significant change in the chemical structure of PAni due to incorporation of the inorganic particles into the polymer matrix. In Figure 1a [(2) and (3)], it can be seen that the two bands of AsW_9O_{33} at 711 cm^{-1} and 767 cm^{-1} equally assigned to ν_{as} W−O_c−W are overlapped with the C−H out-of-plane bending mode of PAni. In addition, two well distinct bands corresponding to ν_{as} As−O_a and ν_{as} W−O_d also appeared at 889 cm^{-1} and 967 cm^{-1}, respectively. On closer examination, the spectra of PAni@AsW_9O_{33} materials obtained

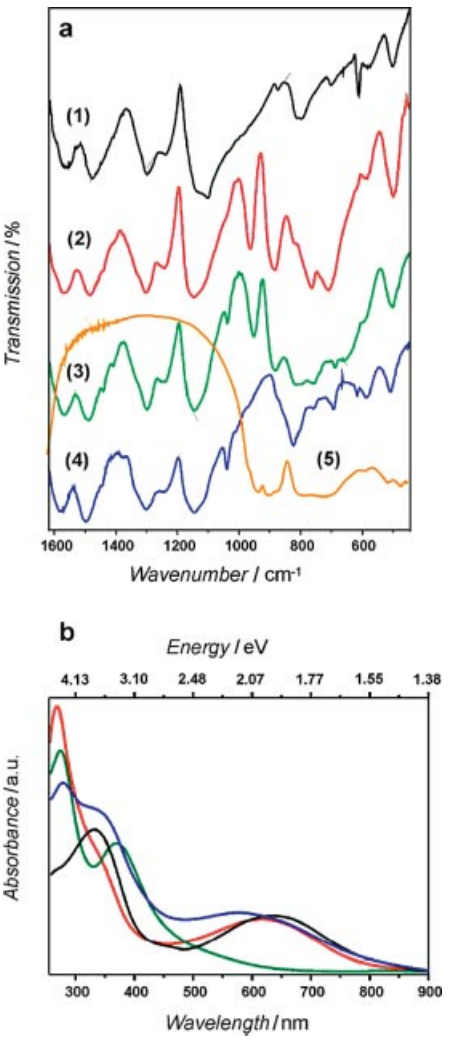

Figure 1. (a) FTIR spectra of (1) pristine PAni prepared in acidic media; (2) PAni@AsW_9O_{33} prepared in acidic media; (3) PAni@AsW_9O_{33} obtained from aqueous media; (4) pristine PAni prepared in aqueous media; (5) pure $Na_9[AsW_9O_{33}]\cdot 16H_2O$; (b) UV/Vis spectra of pristine PAni synthesized in acidic media (black), pristine PAni obtained from aqueous media (blue), PAni@AsW_9O_{33} synthesized in acidic media (red) and PAni@AsW_9O_{33} obtained from aqueous media (green).

from aqueous and acidic media, respectively, display differences in the W−O_c−W bridge stretching region. In particular, the region is broadened with three bands at 694 cm^{-1}, 762 cm^{-1} and 804 cm^{-1} and is almost engulfing the ν_{as} As−O_a [Figure 1a (3)] in the spectra of the hybrid material synthesized in aqueous solution; in contrast to the two bands of the counterpart from acidic media and the pure $[AsW_9O_{33}]^{9-}$. The band broadening may suggest a symmetry decrease of the $[AsW_9O_{33}]^{9-}$ from a lower oxidation state to a higher one [40].

The redox state of PAni alongside the structural modification due to the incorporation of inorganic components into the polymer can be elucidated by UV/Vis spectroscopy as shown in Figure 1b. The spectrum of the pure polymer prepared in the acidic system shows two major absorption

Zeitschrift für anorganische und allgemeine Chemie ZAAC Journal of Inorganic and General Chemistry

peaks at about 329 nm and 635 nm. The similarity in the absorbance of the samples with and without extra $CHCl_3$ purification is in agreement with our earlier IR analysis, which shows that the additional purification step with $CHCl_3$ has no significant influence on the chemical structure of the polymer that was isolated from an acidic reaction medium (cf. Supporting Information, Figure 2s). The high energy peak at 329 nm is assigned to the $\pi-\pi^*$ transition of the benzenoid rings which relates to the extent of conjugation between adjacent phenyl rings in the polymer chain, while the lower energy peak at 635 nm is assigned to the exciton absorption of the quinoid rings, attributed to the intrachain or interchain charge transport [41−43]. Comparatively, the spectra of the pure polymer obtained from the aqueous system exhibits a hypsochromic shift in the exciton absorption to Peierls bandgap (~2.2 eV), which emanates from ring torsion and bond length dimerization (Figure 1b) [43−45]. It can also be seen that there is a bathochromic shift of the $\pi-\pi^*$ transition when the oligomers are not washed off with chloroform (Figure 2s). In general, the spectra of PAni synthesized in water-based solutions exhibit an additional peak below 300 nm (~ 4.5 eV), which is unaffected by $CHCl_3$ purification and is absent in the spectra of PAni prepared in acidic media. The appearance of more absorption peaks might be suggesting a higher conjugated system. The encapsulation of $[AsW_9O_{33}]^{9-}$ by the PAni host via the two different media brought forward a preparation-dependent change in the redox state and chemical structure of the polymer (Figure 1b). In the spectra of the PAni@AsW_9O_{33} obtained from acidic systems, it can be seen that the molecular exciton absorption is shifted towards the Peierls gap while the $\pi-\pi^*$ transition disappeared and a new absorption peak is observed below 300 nm. This is possibly due to the oxidation of polyaniline by the nonatungstoarsenate(III) to a highly oxidized state (pernigraniline) that exhibits Peierls distortion and diminished $\pi-\pi^*$ transition; the new peak is a consequence of the embedded inorganic nanoparticles that absorb in the higher energy region (~ 4.4 eV). On the other hand, the spectra of PAni@AsW_9O_{33} synthesized in water exhibit a hyperchromic absorption of both $\pi-\pi^*$ transition and the high-energy peak (~ 4.5 eV) with a complete disappearance of the molecular exciton absorption. This is typical for the reduced state of polyaniline (leucoemeraldine) [43] and implies that $[AsW_9O_{33}]^{9-}$ is probably oxidized to a higher state in this aqueous reaction system, supporting our earlier allusion founded on the IR analysis. Based on these observations, we infer that the redox state of PAni is altered by the lacunary Keggin-type polyoxotungstoarsenate $[AsW_9O_{33}]^{9-}$ depending on the synthetic media.

Morphology and Properties

The presence of $[AsW_9O_{33}]^{9-}$ in PAni is further verified by the X-ray diffraction analysis. Whereas pristine PAni exhibits three major peaks around ~ 19°, 25° and 42°, the incorporation of $[AsW_9O_{33}]^{9-}$ leads to significant changes in the relative intensities and peak positions (cf. Figure 3s) as well as to the appearance of more pronounced low-angle reflections.

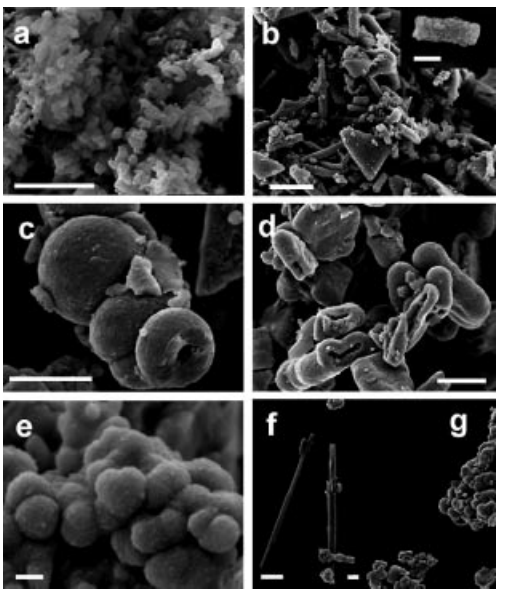

Figure 2. (a) Pristine PAni obtained from acidic reaction media and (b) pristine PAni synthesized in aqueous solution (scale bar = 1 μm, inset = 200 nm); (c, d) PAni@AsW_9O_{33} synthesized in aqueous reaction systems (scale bar = 1 μm); (e) spherical (scale bar = 100 nm) and (f, g) rod-shaped PAni@AsW_9O_{33} synthesized in acidic reaction systems (scale bar = 300 nm).

Figure 2 shows the cryogenic scanning electron microscopy (cryo-SEM) images of powdered samples of PAni and the derived PAni@AsW_9O_{33} hybrids. The different synthetic media exert an influence on both the size and the morphology of the products. Generally, in acidic systems, the pristine polymers (Figure 2a, b) tend to form short rods with diameters in the size range of 40 to 95 nm whereas longer rods with diameter sizes of less than 200 nm are formed by aggregates of spherical particles in the aqueous system.

A spectrum of different submicron morphologies of the as-synthesized powdered samples is observed for both reaction pathways. Figure 2c shows a typical image of spherical aggregates with diameters in a broad size range of less than 1 μm for the hybrid grown in aqueous media. Closer examination of the images reveals that many of the spherical structures and of the other irregular shaped aggregates appear to be hollow. This is possibly due to the growth of the polymer in the presence of nonatungstoarsenate (III) in the aqueous system. In contrast, the hybrids prepared in the acidic system (Figure 2e−g) do not display a comparable porous morphology. Instead, rather discrete long rods as well as spherical and irregular block-shaped aggregates with varying diameters below 550 nm are formed. We have found that pellets of the hybrids isolated from the water-based reaction system are fragile as compared to their acidic counterparts, which could be a consequence of the porous morphologies, possibly ensuing from the weaker

interaction between the monomer and the inorganic particles during the preparation in the aqueous system. Furthermore, we observed that neither the synthesis time nor the extra purification step with $CHCl_3$ exerts an obvious effect on the size and morphology of the particles.

The successful incorporation of nonatungstoarsenate(III) into PAni is further confirmed by the energy-dispersive X-ray (EDX) analyses of the hybrids obtained from the two different systems (Figure 3).

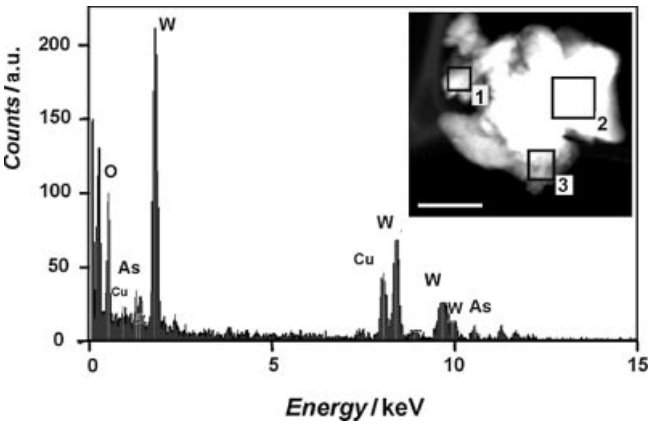

Figure 3. STEM image (inset with spots indicating EDX analyses, scale bar = 500 nm) and a representative EDX spot analysis of PAni@AsW_9O_{33}.

The presence of elemental arsenic, tungsten and oxygen in the EDX spectrum proves that nonatungstoarsenate(III) is embedded in the polymer matrix. However, the sodium content cannot be determined with this methodology. EDX of the residual mass obtained from the thermogravimetric analyses (TGA) of the hybrids reveals that elemental arsenic is absent after complete decomposition of the polymer at ca. 700 °C (Figure 4). Both XRD patterns and FTIR/UV/Vis spectra confirm that the residual mass consists only of tungsten oxide. The analysis of the residue obtained from the TGA of pure $Na_9[AsW_9O_{33}]\cdot 16H_2O$ led to analogous results, affirming that elemental arsenic is no longer present due to the volatile nature of arsenic oxides at high temperatures. TGA shows that the inorganic particles have no noticeable impact on the thermal stability of the polymer than pristine PAni – both materials start to decompose between 300 and 400 °C.

The temperature dependence of the electrical resistivity, $\rho(T)$, of different samples is shown in Figure 5. As outlined above, the samples were not doped with any acid after the synthesis and rigorous purification stage(s). The structural properties as evaluated by our several characterization techniques can be readily correlated to the resistivity of the materials. As expected, the $\rho(T)$ of the samples prepared in the acidic media are lower than that of the materials obtained via the aqueous system for all samples under investigation. In the acidic reaction system, there is an increase in resistivity of the hybrid in comparison to that of the pristine polymer, which corresponds to the higher bandgap energy prevalent in the hybrids as elucidated by the UV/Vis studies

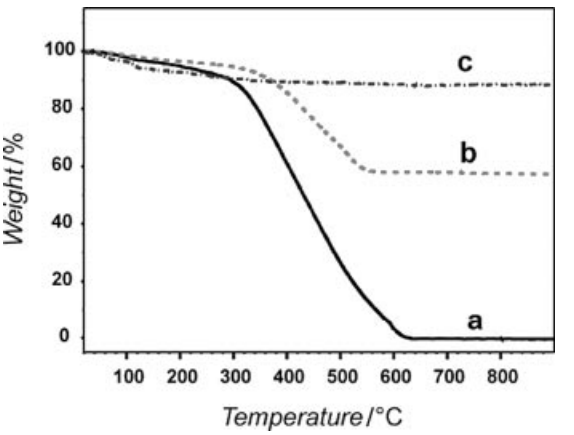

Figure 4. Thermogravimetric analysis of PAni (a), PAni@AsW_9O_{33} (b) and AsW_9O_{33} (c).

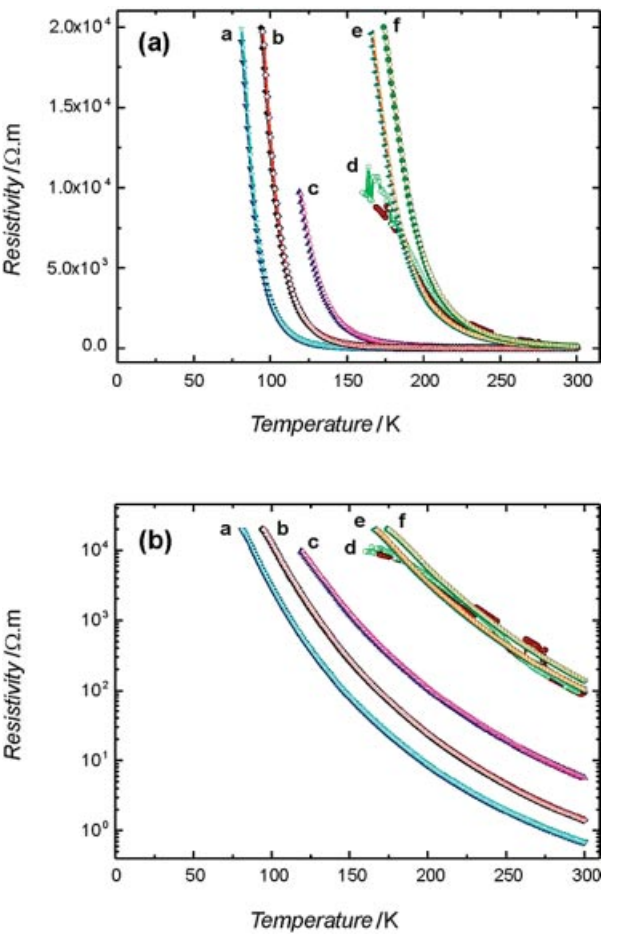

Figure 5. (**a** = linear plot, **b** = logarithmic plot): Resistivity temperature dependence for a) pristine PAni isolated from acidic media without $CHCl_3$ purification and b) with additional $CHCl_3$ purification; c) PAni@AsW_9O_{33} synthesized in acidic reaction systems; d) pristine PAni obtained from water-based systems without $CHCl_3$ purification and e) with $CHCl_3$ purification; f) PAni@AsW_9O_{33} obtained from aqueous media.

(Figure 1b). This is somewhat in contrast to the aqueous reaction system where the hybrid displays resistivity akin to the pristine PAni. In general, we observed a slight increase

Zeitschrift für anorganische und allgemeine Chemie ZAAC Journal of Inorganic and General Chemistry

in the resistivity of the samples purified additionally with $CHCl_3$, which suggests little deprotonation of the samples. The plots show that the resistivity of the materials increases steadily on cooling down to lower temperatures. Except for the hybrid material arising from the water-based system, it can also be seen in the plots that there is no obvious difference in the resistivity of the materials during cooling (Figure 5: closed symbols) and warm-up measurements (Figure 5: open symbols).

This suggests that the samples are stable and are able to withstand the cooling and heating treatments during the measurements under vacuum conditions. The changes observed for the hybrid prepared in the aqueous system may be related to the porous structure as already discussed above and could suggest crack formations, typical of an instability of the material during the electrical measurements. However, in general, the reproducible resistivity curve of the materials during cooling and warm-up measurements over a wide temperature range is prerequisite for their use as smart materials.

Conclusions

In summary, we have demonstrated the incorporation of the lacunary lone-pair containing Keggin anion $[AsW_9O_{33}]^{9-}$ into polyaniline via two different synthetic strategies. The alternative approaches offer the preparation of pristine PAni and the derived hybrids with varying structural, optical and electronic properties. Additional purification of PAni with chloroform is essential when the synthesis is carried out in aqueous media. The lone-pair containing lacunary polyoxoanion, depending on the synthetic media, could alter the redox state of PAni and as well induce a nanoscale structuring of PAni, varying from rod-shaped structures obtained in acidic media to hollow submicron structures resulting from syntheses performed in aqueous media. The steady to-cool down and fro-warm up electrical behavior of the materials over a wide temperature range is a good starting point for their direct application as novel and flexible materials, e.g. in actuators. Further investigations on the resistivity of the POM-PAni hybrids are in progress. The synthetic strategy outlined in this work is currently applied upon the incorporation of more complex POMs with interesting magnetic properties into the PAni matrix.

Experimental Section

Materials

Aniline (99.5 + %), ammonium persulfate (98 + %) and *N*-methyl-2-pyrrolidone (99 + %) were all purchased from Sigma-Aldrich and used as received. $Na_9[AsW_9O_{33}]\cdot 16H_2O$ was prepared according to the literature [46]. Sulfuric acid was obtained as a concentrated solution from Merck. Chloroform stabilized with ethanol (99.47 %) was purchased from Scharlau. Deionized water was used for all experimental procedures.

Preparation of PAni@AsW_9O_{33} and PAni

A sample of $[AsW_9O_{33}]^{9-}$ (0.12 mmol) was completely dissolved in either water or sulfuric acid (0.5 M). Aniline (1.3 mmol) was subsequently added to the solution and the mixture was stirred magnetically for 1−2 h. A solution of ammonium persulfate (1.8 mmol) in either water or H_2SO_4 was then added to the corresponding mixture and the polymerization was allowed to proceed without stirring at room temperature for 2−6 h. The products were isolated by filtration, thoroughly washed with deionized water and dried at 65 °C. The additional purification step was carried out by soaking considerable amount of the dried samples in chloroform for 6−9 h with intermittent agitation. The samples were thereafter filtered, repeatedly washed with the same solvent and dried at 65 °C for 72 h.

Characterization

Fourier transform infrared (FT-IR) spectra were recorded with a Perkin-Elmer BXII spectrometer with KBr pellets. Samples were freeze-etched for cryo-electron microscopy in a BAF 060 freeze-etching device (Fa. Bal-Tec, Balzers, Liechtenstein) and coated with a thin layer of tungsten. Cryo-scanning electron microscopy (SEM) was performed with a LEO 1530 (FEG) microscope equipped with a cryo stage (Fa. Bal-Tec, Balzers, Liechtenstein). X-ray diffractograms were recorded in reflection mode (flat sample holders) with a Bruker AXS D8 diffractometer using Cu-K_α radiation. UV/Vis spectra of dilute solutions of the samples in *N*-methyl-2-pyrrolidone (NMP) were recorded with a Cary 500 Scan with a 1 mm cuvette. TGA-DTA analysis of the samples was carried out with a Netzsch STA 449C at a heating rate of 10 °C min^{-1} under a dynamic air flow of 50 cm^3 min^{-1}. The scanning transmission electron microscopy (STEM) images were recorded with a HAADF detector on a FEI Tecnai F30 microscope, operated at 300 kV (field emission cathode). In the STEM mode, the electron beam was placed on a selected spot, and an elemental analysis by energy-dispersive X-ray spectroscopy (EDS, EDAX detector) was performed. Resistivity measurements were performed with the four-point probe method on gold patterned pressed pellets of the samples using the Quantum Design Physical Property Measurement System, at temperatures in the range of 10 to 300 K. Silver glue paint was used to attach the electrical contacts.

Supporting Information (see footnote on the first page of this article): FT-IR and UV/Vis spectra of PAni synthesized under different conditions, XRD patterns of PAni@AsW_9O_{33} and PAni.

Acknowledgement

The authors acknowledge support of the Electron Microscopy ETH Zurich, EMEZ. We thank *Dr. Roger Wepf*, EMEZ, for Cryo-SEM analyses and *Dr. Frank Krumeich*, EMEZ, for STEM and EDX analyses. Financial support by the *Swiss National Science Foundation* (SNF Professorship PP002-114711/1) and by the *University of Zurich* is gratefully acknowledged.

References

[1] R. Gangopadhyay, A. De, *Chem. Mater.* **2000**, *12*, 608.
[2] a) G. Kickelbick, *Prog. Polym. Sci.* **2003**, *28*, 83; b) K. Landfester, *Annu. Rev. Mater. Res.* **2006**, *36*, 231; c) S. Meuer, P. Oberle, P. Theato, W. Tremel, R. Zentel, *Adv. Mater.* **2007**, *19*, 2073.

[3] H. Cölfen, M. Antonietti, *Angew. Chem. Int. Ed.* **2005**, *44*, 5576.
[4] F. Hoffmann, M. Cornelius, J. Morell, M. Fröba, *Angew. Chem. Int. Ed.* **2006**, *45*, 3216.
[5] S. Hartmann, D. Brandhuber, N. Hüsing, *Acc. Chem. Res.* **2007**, *40*, 885.
[6] S. Virji, J. X. Huang, R. B. Kaner, B. H. Weiller, *Nano Lett.* **2004**, *4*, 491.
[7] a) J. H. Burroughes, D. D. C. Bradley, A. R. Brown, R. N. Marks, K. Mackay, R. H. Friend, P. L. Burns, A. B. Holmes, *Nature* **1990**, *347*, 539; b) D. Braun, A. J. Heeger, *Appl. Phys. Lett.* **1991**, *58*, 1982.
[8] a) J. Joo, C. Y. Lee, *J. Appl. Phys.* **2000**, *88*, 513; b) C. Y. Lee, H. G. Song, K. S. Jang, E. J. Oh, A. J. Epstein, J. Joo, *Synth. Met.* **1999**, *102*, 1346.
[9] F. Treptow, A. Jungbauer, K. Hellgardt, *J. Membr. Sci.* **2006**, *270*, 115.
[10] a) T. G. Backlund, H. G. O. Sandberg, R. Osterbacka, H. Stubb, T. Makela, S. Jussila, *Synth. Met.* **2005**, *148*, 87; b) P. S. Barker, A. P. Monkman, M. C. Petty, R. Pride, *Synth. Met.* **1997**, *85*, 1365.
[11] A. K. Cuentas-Gallegos, M. Lira-Cantú, N. Casañ-Pastor, P. Gómez-Romero, *Adv. Funct. Mater.* **2005**, *15*, 1125.
[12] B. Keita, A. Belhouari, L. Nadjo, R. Contant, *J. Electroanal. Chem.* **1995**, *381*, 243.
[13] M. T. Pope, *Heteropoly- and Isopolyoxometalates*, Vol. 8, Springer-Verlag, Berlin **1983**.
[14] M. T. Pope, A. Müller (Eds.), *Polyoxometalates: From Platonic Solids to Anti-Retroviral Activity*, Kluwer Academic Publishers, Dordrecht **1994**.
[15] T. Yamase, M. T. Pope, *Polyoxometalate Chemistry for Nano-composites Design*, Kluwer Academic Publishers, Dordrecht **2002**.
[16] C. L. Hill, *Chem. Rev.* **1998**, *98*, 1.
[17] S. Roy, M. C. D. Mourad, M. T. Rijneveld-Ockers, *Langmuir* **2007**, *23*, 399.
[18] J. F. Keggin, *Nature* **1933**, *132*, 351.
[19] J. F. Keggin, *Proc. R. Soc. London, Ser. A* **1934**, *144*, 0075.
[20] Y. Gao, S. Yao, J. Gong, L. Y. Qu, *Macromol. Rapid Commun.* **2007**, *28*, 286.
[21] J. Vaillant, M. Lira-Cantú, K. Cuentas-Gallegos, N. Casañ-Pastor, P. Gómez-Romero, *Prog. J. Solid State Chem.* **2006**, *34*, 147.
[22] P. Gómez-Romero, M. Chojak, K. Cuentas-Gallegos, J. A. Asensio, P. J. Kulesza, N. Casañ-Pastor, M. Lira-Cantú, *Electrochem. Commun.* **2003**, *5*, 149.
[23] F. Wang, X. Xu, J. Gong, Y. Luo, Y. Hou, X. Zheng, L. Qu, *Mater. Lett.* **2005**, *59*, 3982.
[24] P. S. Kishore, B. Viswanathan, T. K. Varadarajan, *Nanoscale. Res. Lett.* **2008**, *3*, 14.
[25] G. Bidan, M. Lapkowski, J. P. Travers, *Synth. Met.* **1989**, *28*, C113.
[26] P. Gómez-Romero, N. Casañ-Pastor, M. Lira-Cantú, *Solid State Ionics* **1997**, *101–103*, 875.
[27] M. Lira-Cantú, P. Gómez-Romero, *Chem. Mater.* **1998**, *10*, 698.
[28] P. J. Kulesza, M. Chojak, K. Miecznikowski, A. Lewera, M. A. Malik, A. Kuhn, *Electrochem. Commun.* **2002**, *4*, 510.
[29] Y. Wang, C. Guo, Y. Chen, C. Hu, W. Yu, *J. Colloid Interface Sci.* **2003**, *264*, 176.
[30] M. Barth, M. Lapkowskia, S. Lefrant, *Electrochim. Acta* **1999**, *44*, 2117.
[31] Y. Wang, X. Wang, C. Hu, C. Shi, *J. Mater. Chem.* **2002**, *12*, 703.
[32] D. G. Kurth, D. Volkmer, M. Ruttorf, B. Richter, A. Müller, *Chem. Mater.* **2000**, *12*, 2829.
[33] U. Kortz, N. K. Al-Kassem, M. G. Savelieff, N. A. Al Kadi, M. Sadakane, *Inorg. Chem.* **2001**, *40*, 4742.
[34] F. Hussain, R. W. Gable, M. Speldrich, P. Kögerler, C. Boskovic, *Chem. Commun.* **2009**, 328.
[35] W. Chen, Y. Li, Y. Wang, E. Wang, Z. Su, *Dalton Trans.* **2007**, 4293.
[36] J. Laska, J. Widlarz, *Polymer* **2005**, *46*, 1485.
[37] U. Kortz, M. G. Savelieff, B. S. Bassil, B. Keita, L. Nadjo, *Inorg. Chem.* **2002**, *41*, 783.
[38] M. Bosing, I. Loose, H. Pohlmann, B. Krebs, *Chem. Eur. J.* **1997**, *3*, 1232.
[39] E. T. Kang, K. G. Neoh, K. L. Tan, *Prog. Polym. Sci.* **1998**, *23*, 277.
[40] C. Rocchiccioli-Deltcheff, R. Thouvenot, *J. Chem. Res. (S)* **1977**, 46.
[41] S. Stafstrom, J. L. Bredas, A. J. Epstein, H. S. Woo, D. B. Tanner, W. S. Huang, A. G. MacDiarmid, *Phys. Rev. Lett.* **1987**, *59*, 1464.
[42] J. E. de Albuquerque, L. H. C. Mattoso, R. M. Faria, J. G. Masters, A. G. MacDiarmid, *Synth. Met.* **2004**, *146*, 1.
[43] J. G. Masters, J. M. Ginder, A. G. MacDiarmid, A. J. Epstein, *J. Chem. Phys.* **1992**, *96*, 4768.
[44] R. Mackenzie, J. M. Ginder, A. J. Epstein, *Phys. Rev. B* **1991**, *44*, 2362.
[45] J. M. Ginder, A. J. Epstein, A. G. MacDiarmid, *Synth. Met.* **1991**, *43*, 3431.
[46] C. Tourné, A. Revel, G. Tourné, M. Vendrell, *C. R. Acad. Sci. Ser. C* **1973**, *277*, 643.

Received: December 18, 2008
Published Online: February 11, 2009

